JOURNAL OF AIRCRAFT
Vol. 40, No. 1, January–February 2003

Compressibility and Excitation Location Effects on High Reynolds Numbers Active Separation Control

Avi Seifert*
Tel-Aviv University, 69978 Ramat Aviv, Israel
and
LaTunia G. Pack†
NASA Langley Research Center, Hampton, Virginia 23681

The effects of compressibility and excitation slot location on active separation control at high Reynolds numbers are explored. The model, which was tested in a cryogenic pressurized wind tunnel, simulates the upper surface of a 20% thick Glauert–Goldschmied-type airfoil at zero angle of attack. The boundary layers on the model are turbulent because the tunnel sidewall boundary layer flows over it. Without control, the flow separates at the highly convex area of the model and a large turbulent separation bubble is formed. Periodic excitation was applied to control the separation bubble. Two alternative blowing slot locations, as well as the effect of compressibility and steady suction or blowing, were studied. During the test, the chord Reynolds numbers ranged from 1.1×10^7 to 3×10^7 and the Mach numbers ranged from 0.25 to 0.7. It was found that excitation must be introduced slightly upstream of the separation region at low Mach number. Introduction of excitation upstream of the shock wave is more effective than at its foot. Compressibility reduces the ability of steady mass transfer and periodic excitation to control the separation bubble, but periodic excitation has an effect on the integral parameters, which is similar to that observed in low Mach numbers. Blowing becomes more effective than suction at transonic speeds, whereas the opposite was found in low Mach numbers. The data presented provide a proper validation case for unsteady numerical design tool that will enable exploring the full potential of unsteady flow control.

Nomenclature

C_{dp}	=	pressure drag coefficient
C_m	=	moment coefficient
C_n	=	normal force coefficient
C_p	=	wall pressure coefficient, $(P - P_s)/q$
$C_{p,\min}$	=	minimum pressure coefficient
C_μ	=	combined blowing momentum coefficient, $(c_\mu; \langle c_\mu \rangle)$
c	=	model chord
c_μ	=	steady blowing momentum coefficient, J/cq
$\langle c_\mu \rangle$	=	oscillatory blowing momentum coefficient, $\langle J' \rangle / cq$
F^+	=	reduced frequency, $(f x_{sp})/U_\infty$
f	=	oscillation frequency, Hz
h	=	slot height or width
J	=	momentum at slot exit, $\rho h U_j^2$
M	=	Mach number
P	=	pressure
q	=	freestream dynamic pressure, $1/2\rho U_\infty^2$
R_c	=	chord Reynolds number, $U_\infty c/\nu$
T	=	temperature
U, u	=	average and fluctuating streamwise velocity
X_{sp}	=	distance from baseline separation to reattachment
x/c	=	normalized streamwise location
z	=	spanwise location
$\Delta C_{p,rec}$	=	pressure rise from $C_{p,\min}$ to $C_{p,s}$
ν	=	kinematic viscosity
ρ	=	density
$\langle\,\rangle$	=	phase locked values

Subscripts

b	=	baseline flow conditions
c	=	cavity
crit	=	sonic conditions
d	=	derectified hot-wire data
j	=	conditions at blowing slot
N	=	normalized according to text
R	=	reattachment
S	=	separation
∞	=	freestream conditions

Superscript

$'$	=	root mean square of fluctuating value

I. Introduction

BOUNDARY-LAYER control (BLC) research dates back to the turn of the 20th century, for example, that of Prandtl (see Ref. 1). However, low efficiency, complexity, and maintenance difficulties prevented the utilization of laboratory-proven BLC techniques, such as blowing or suction. Forced oscillations superposed on a mean flow that is on the verge of separating are very effective in delaying turbulent boundary-layer separation.[2] Experiments performed on various existing airfoils at low and high Reynolds numbers[3–5] demonstrated that even if the flow is not fully attached, the lift could be significantly enhanced by the introduction of periodic excitation into the separated shear layer. This is achieved by exciting the flow at frequencies that generate from two to four spanwise coherent vortices over the length of the separated region, that is, $F^+ \approx 1$. The periodic excitation increases the momentum transfer across the shear layer, enhancing its resistance to separation under an adverse pressure gradient. The technique was also demonstrated at high Reynolds number, compressible speeds.[6] Though demonstrated experimentally, active separation control using periodic excitation is still a challenge for numerical simulation, and design tools are not available.

The appropriate use of active BLC should enable simplified, cheaper, more efficient, and more reliable systems, while

Received 6 March 2002; revision received 27 August 2002; accepted for publication 4 September 2002.

*Senior Lecturer, Department of Fluid Mechanics and Heat Transfer, Faculty of Engineering. Associate Fellow AIAA.
†Research Engineer, Flow Physics and Control Branch. Member AIAA.

maintaining performance. A multidisciplinary design optimization process should allow simplified high-lift systems, thicker airfoils with lighter structures and greater internal volume, shorter aft bodies, size reduction, and even elimination of conventional control surfaces. Existing design tools are capable of reproducing steady flows, including steady mass transfer, but the inclusion of unsteady BLC effects into computational fluid dynamics (CFD) tools has not been performed yet. The development of a proper CFD design tool is dependent on the availability of a comprehensive database at relevant conditions, that is, flight Reynolds numbers, to allow its validation.

Flow separation at compressible speeds typically occurs downstream of a shock-wave/boundary-layer interaction. The pressure jump across the shock either causes immediate separation or thickens the boundary layer and reduces its momentum such that it separates further downstream. Once the flow separates downstream of the shock, the unsteady separation and subsequent reattachment (if it occurs) induce unsteadiness in both the shock position and strength. This phenomenon is known as buffeting. The low-frequency oscillations can cause structural damage, if coupled with the resonance frequencies of the structure. Several passive methods for controlling compressible separation exist,[7] and unsteady BLC at compressible speeds was demonstrated[6] on a NACA 0015 airfoil. Introduction of periodic excitation upstream of the shock wave improved the performance of the airfoil and reduced the unsteadiness in its wake.

The present experiment is intended to supplement the airfoil experiment[6] by providing additional flexibility in the control parameters and more detailed measurements of the mean and fluctuating wall pressures, allowing improved understanding of controlling separated flows at flight Reynolds number compressible speeds and providing a comprehensive database for validation of unsteady CFD design tools. Effects due to the location for introduction of the control input are also considered over a wide range of Mach numbers. A previous publication[8] presented some of the experimental results for incompressible two-dimensional flow over the same model. Section II of this paper provides a brief description of the experimental setup. Section III presents the experimental results, initially of the baseline flow and, thereafter, those of the controlled flow and the effect of the excitation slot location.

II. Description of the Experiment

The setup of the experiment was described in detail in a previous publication.[8] Only vital details will be provided here.

A. Hump Model

The model simulates the upper surface of a 20% thick, Glauert–Goldschmied-type airfoil (see Ref. 8). The model, with a reference chord of 200 mm, was installed on the right-side tunnel turntable. The original location of the airfoil leading edge is defined as the reference leading edge (Fig. 1). This area was faired smoothly from $x/c = -0.05$ to 0.05 to eliminate a slope discontinuity. Two alternative excitation slot locations are available: $x/c = 0.59$ and 0.64. The position of the upstream slot was selected such that it would be upstream of the expected position of a shock wave. The slots were about 0.25% chord wide (0.50 ± 0.05 mm) and allowed an

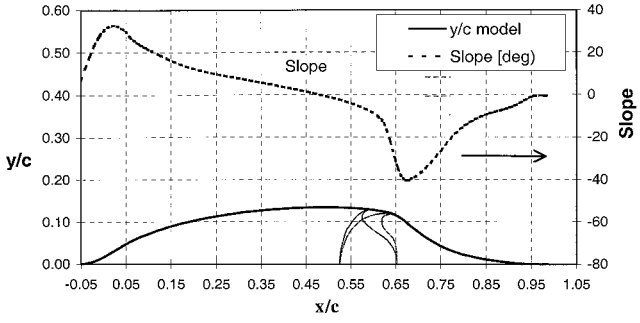

Fig. 1 Cross section of the hump model, as mounted on the tunnel sidewall; actuator cavity shown centered on $x/c = 0.6$ with the two alternative slot locations.

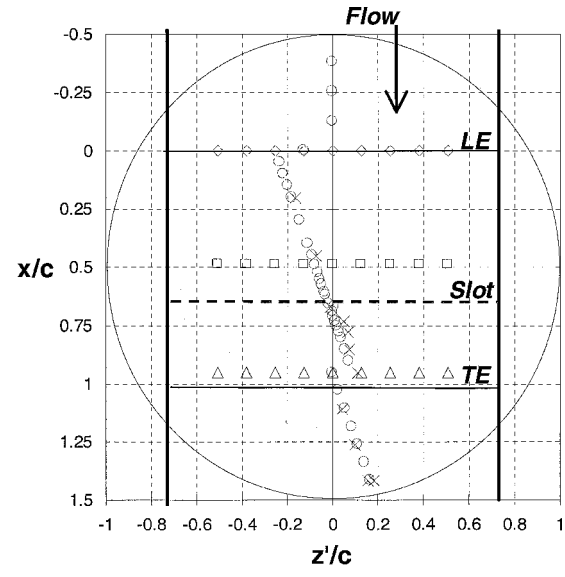

Fig. 2 Top view of the hump model: ||, location of the end plates; ×, unsteady pressure sensors; and other symbols, static pressure taps.

almost tangential downstream introduction of momentum (Fig. 1). The floor and ceiling boundary layers did not affect the spanwise uniformity of the flow over the model that is installed on the sidewall, due to the use of a pair of end plates (vertical thick lines in Fig. 2). The gap between the end plates and the tunnel walls was 12.7 mm, which was deemed sufficient based on the available wind-tunnel boundary-layer data.[9] Data acquired during this experiment[8] verify that this gap was sufficient. The tunnel cross-sectional blockage due to the model and end plates is 0.0836. The distribution of the pressure taps is also shown in Fig. 2. The internal diameter of all pressure tap orifices was 0.254 mm. The model was also instrumented with 12 unsteady pressure transducers (indicated by × symbols on Fig. 2). The transducers are installed under the model surface, inside small-volume cavities. The cavities are connected to the surface of the model by 0.254-mm-diam orifices. The effect of this installation on the frequency response of the unsteady pressure transducers is complex, and it was studied using a comprehensive bench-top calibration. In addition, one transducer was flush mounted near the trailing edge of the turntable next to a recessed pressure transducer, and its readings are compared to those of a recessed pressure transducer. One unsteady pressure transducer was installed inside the model cavity, midway between the end plates and about 30 mm from the slot exit. It is used to monitor the cavity pressure oscillations in the wind tunnel and to correlate the wind-tunnel data with the bench-top calibration[8] of the slot exit velocity vs the imposed cavity pressure oscillations.

B. 0.3-Meter Transonic Cryogenic Wind Tunnel

The experiment was conducted in the 0.3-Meter Transonic Cryogenic Wind Tunnel at the NASA Langley Research Center. It is a closed-loop, fan-driven tunnel with a test cross section of 0.33 by 0.33 m. The tunnel operates at stagnation pressures ranging from 1.2 bar up to 6 bar and total temperatures from 78 up to 327 K (Refs. 10 and 11), using gaseous nitrogen is the test medium. A fully automatic control system maintains the test conditions, providing a high level of repeatability. The floor and ceiling of the tunnel were slightly diverged near the model to reduce blockage resulting from boundary-layer growth on the test section walls. In certain runs, a turntable that was instrumented with static pressure orifices was placed opposite the test model to evaluate wall interference.

C. Oscillatory Blowing System

The oscillatory blowing system is capable of generating a wide range of combinations of steady and periodic momentum transfer between the cavity inside the model and the external flow. More details can be found in Ref. 8.

D. Bench-Top Experiments

A bench-top calibration was performed to correlate the fluctuating slot velocities $u'_{j,d}$ with the cavity pressure fluctuations p'_c. This calibration was performed for the $x/c = 0.59$ and 0.64 slots and covered the entire frequency range, as well as most of the normalized amplitude $(p'/\rho)_c$ range that was used in the cryogenic wind-tunnel tests. The frequency response of the present excitation system (oscillatory blowing valve–manifold–cavity) is significantly simpler than the one used previously.[5] This allows the generation of a single correlation between $u'_{j,d}$ and $(p'/\rho)_c$ for each slot calibration. The slot width changed by as much as ±10% (0.05 mm) between different runs due to the modular nature of the model and also due to cryogenic cycling. This is accounted for in the uncertainty level of $\langle c_\mu \rangle$, that is, ±25%. More details on the slot calibration are given in Refs. 5, 6, and 8.

The frequency response of the unsteady pressure transducers was modified due to the difference in the installation of individual transducers. To quantify this effect, all of the transducers underwent a bench-top calibration, before installation and as installed in the model, at ambient conditions. This was performed with the model outside the test section as well as when the model was installed in the tunnel. A sound source and a microphone were placed close to the model. The output of all transducers and the microphone were recorded. The correction procedure is temperature dependent[6] because the resonance frequency is proportional to $\sqrt{(T_{\text{wind tunnel}}/T_{\text{bench top}})}$. Because the majority of the installed sensors resonated at a frequency of about 2.5 kHz, and the frequency response up to 2 kHz was flat, only the flat portion of the frequency range is presently considered.

E. Experimental Uncertainty

Most of the experiments were conducted at cryogenic pressurized conditions (at $T \approx 100$ K), close to the lower limit of the tunnel capability. Most of the data were obtained with separated flow regions on or downstream of the model. Table 1 contains the relevant information regarding experimental uncertainties. These values were calculated using ±3 standard deviations of the various experimental conditions and calculated parameters (including repeated runs). All of the test instruments were operated with valid calibrations. The uncertainty of the calculated aerodynamic parameters at $M = 0.25$ are listed in Table 2 (in absolute values and related to flow condition on the model):

These values typically increase in a proportional manner with the increase in the Mach number and should be roughly doubled for $M = 0.65$ data.

Table 1 Uncertainty of flow and control parameters

Item	Uncertainty, % of full scale	Full scale and condition
Slot width	10	0.5 mm
Static temperature	0.3	300 K
Static pressure	0.25	77 psi
R_c	1	$M > 0.2$
M	2	$M < 0.3$
F^+	2	2
c_μ	0.01 or 10	The larger
$\langle c_\mu \rangle$	25	Local values
f	0.3	800 Hz
C_p	1	$M < 0.3$
C_p	3	$M = 0.65$
C'_p	15	$M < 0.3$
C'_p	30	$M = 0.65$

Table 2 Uncertainty of aerodynamic parameters

Parameter	Baseline	Controlled
C_n	0.010	0.015
C_{dp}	0.0005	0.0010
C_m	0.005	0.010

F. Experimental Conditions

The experiments were conducted at Mach numbers ranging from 0.25 to 0.70 and chord Reynolds numbers ranging from 11×10^6 to 30×10^6.

III. Results

A. Overview

The results presented in this part of the paper are divided into three sections. The first section describes the effects of compressibility on the baseline flow over the model. The second section describes the controlled flow in compressible flow conditions, and the third section describes effects of the excitation slot location. The Reynolds number, the excitation frequency and magnitude, and the effect of steady mass transfer, are all considered.

B. Compressibility Effects on the Baseline Flow

The Mach number has a significant effect on the flow characteristics over the model, as shown by the integral parameters that are presented in Fig. 3. These data were acquired at three different Reynolds numbers because the available tunnel test conditions do not allow covering the required Mach number range in a single Reynolds number sweep.[10] However, the Reynolds number was shown to have only a weak effect on the flow over the model at incompressible speeds, presumably due to the elimination of laminar/turbulent transition from the problem.[8] Indeed, the smooth transition of the data between the different Reynolds numbers demonstrates that point in compressible flow conditions also (Fig. 3). Consistent, but weak, Mach number effects could be seen at $M \leq 0.6$. For higher Mach numbers, C_n, C_m, and C_{dp} vary rapidly (Fig. 4). The form drag (C_{dp}, pressure, and wave) increases fourfold between $M = 0.6$ and 0.7, and it is doubled between $M = 0.675$ and 0.7, whereas the quarter-chord moment is also doubled in that narrow range of Mach numbers.

The reason for these variations of the integral parameters becomes clear when observing the steady [solid lines, left-hand side (LHS) ordinate] and fluctuating [broken lines, right-hand side (RHS) ordinate] wall pressures for $R_c = 30 \times 10^6$ and a range of Mach numbers (presented in Fig. 5) and observing several flow indicators corresponding to that data, shown in Table 3. The flow at $x/c < 0.2$ (not

Table 3 Several flow indicators of the data shown in Fig. 5

M	$C_{p,\text{crit}}$	$C_{p,\text{min}}$	$\Delta C_{p,\text{rec}}$
0.600	−1.29	−1.08	−0.56
0.625	−1.14	−1.12	−0.62
0.650	−1.01	−1.29	−0.76
0.675	−0.89	−1.56	−0.93
0.700	−0.78	−1.68	−0.70

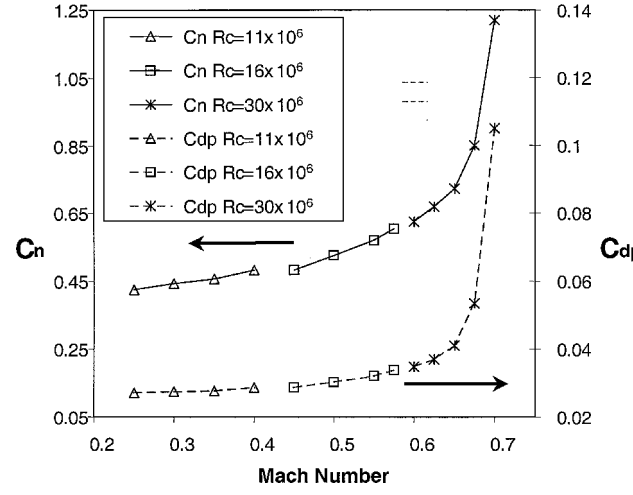

Fig. 3 Baseline integral parameters of the model at compressible flow: ——, C_n and - - - -, C_{dp}.

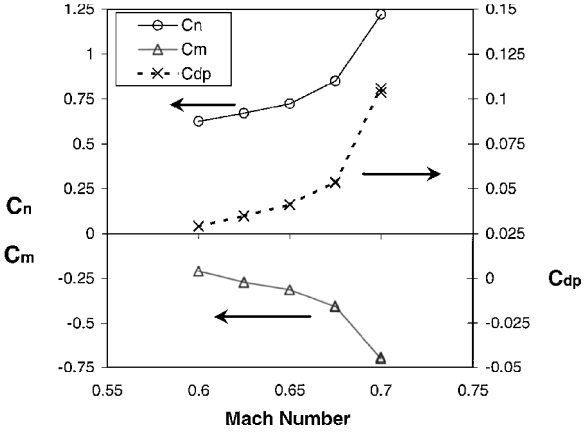

Fig. 4 Baseline integral parameters of the model at compressible flow, $R_c = 30 \times 10^6$.

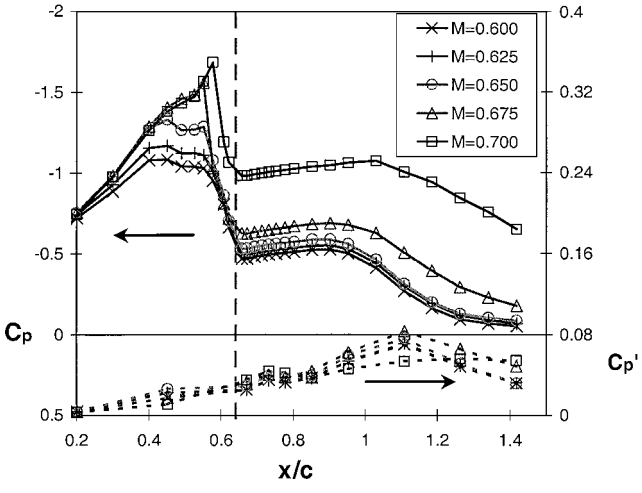

Fig. 5 Mean and fluctuating wall pressures at compressible flow, $R_c = 30 \times 10^6$: ——, C_p with LHS ordinate; ----, C_p' with RHS ordinate; and ⋮, $x/c = 0.64$ slot location.

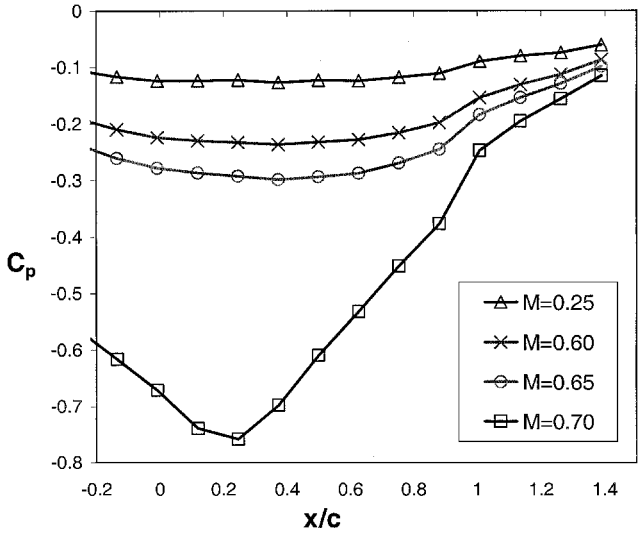

Fig. 6 Mean pressures on the wall opposite the model at compressible flow, $R_c = 30 \times 10^6$.

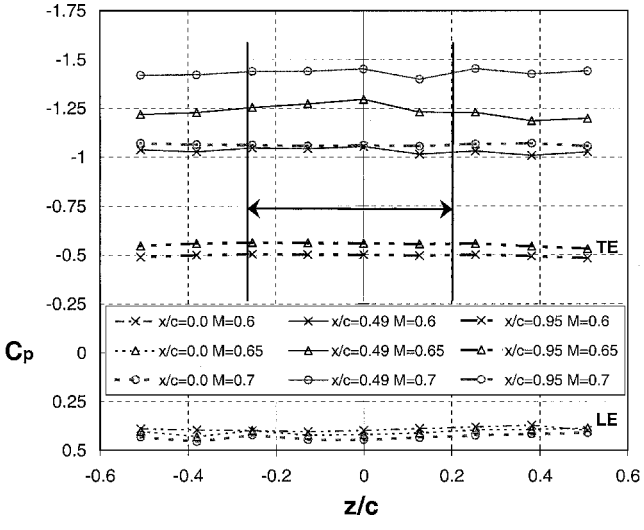

Fig. 7 Spanwise distribution of C_p on the model at compressible flow, $R_c = 30 \times 10^6$.

shown) is insensitive to the Mach number. It was noted that the flow acceleration in the range $0.2 < x/c < 0.5$ increases with the Mach number. This trend started at $M > 0.2$ (not shown). For $M > 0.625$, the flow around the suction peak is supersonic. The sharp pressure rise (recovery), centered on $x/c = 0.6$ at all of the subcritical flow conditions, coincides with the location of the shock wave that terminates the supersonic flow for $M \geq 0.65$. The pressure jump across the shock ($\Delta C_{p,\mathrm{rec}}$, Table 3) increases with M up to $M = 0.675$. Note that C_p at separation decreases as the Mach number increases (again this trend starts for $M > 0.2$), indicative of a limit to the baseline flow pressure recovery of about one. The decrease of C_p at separation as the Mach number increases is the main cause of the integral parameters divergence, which can be seen in Figs. 4 and 5. The negative C_p downstream of reattachment is attributed to tunnel blockage. This is because the reattachment region, as indicated by the location of $C'_{p\,\max}$, does not change for $M < 0.675$ (Fig. 5). The wall pressures opposite the model (plotted in Fig. 6) show that the tunnel blockage increases significantly for $M > 0.65$. Therefore, control was applied at $M = 0.65$, where tunnel wall interference is relatively weak. The shock wave does not turn the flow subsonic at $M = 0.7$ and a supersonic separation takes place (Fig. 5). The flow reattachment for $M < 0.7$ does not change considerably because the separation is subsonic. A good approximation of the reattachment location is one separation height downstream of the location of $C'_{p\,\max}$ (Ref. 8). For $M = 0.7$, the flow reattaches downstream of the measurement domain, and there are indications of buffeting and prohibitively high drag. The effect of the Mach number on the fluctuating wall pressures for $M < 0.675$ is weak, as shown in Fig. 5.

A small downstream movement of $C'_{p\,\max}$ at $M = 0.7$ is indicative of delayed reattachment. The C'_p distribution for $M = 0.7$ differs from the lower Mach numbers in that it does not peak at $x/c \approx 1.1$, but has a lower flat peak centered at $x/c \approx 1.3$. A comparison of the spectral contents at $M = 0.65$ and 0.7 reveals that the power spectral density at the higher Mach number and $F^+ < 1$ increases by about an order of magnitude without showing any distinctive peak in that F^+ range.

The spanwise distributions of C_p at compressible speeds are presented in Fig. 7 (not shown). Note that for $x/c = 0$ and 0.95, the pressures are uniform (± 0.01) at least over the range $z/c = \pm 0.55$. For $x/c = 0.49$, the maximum deviation of the local C_p from the mean C_p across the span is ± 0.03. This larger deviation can be attributed to minute changes in the contour due to the modular nature of the model as well as cryogenic cycling that are manifested as C_p variations in locally supersonic speeds, but overall the spanwise uniformity of C_p was found to be satisfactory.

C. Controlled Flow over the Hump Model

1. *Overview*

This section is devoted to a description of the controlled flow over the hump model. Because the baseline flow contains separated flow, there is no attached baseline flow to be used as a reference. Strong suction was applied to reattach the flow at low Mach numbers, and it

was used to study fully attached flow.[8] At compressible speeds, the available suction or blowing levels were insufficient to fully reattach the flow, or to at least demonstrate saturation of the effect, but the efficacy of steady and oscillatory momentum coefficients could be compared at different Mach numbers. Thereafter, periodic excitation was used to control the size of the separation bubble gradually. The parameters that were modified during the test are the frequency and the amplitude of the periodic excitation, and the magnitude of the steady mass flux. An additional geometrical parameter was the excitation slot location. The effects of the Reynolds and Mach numbers were also studied. The spanwise uniformity of the mean wall pressures was found to be very good (see Fig. 7) and generally improved with the application of periodic excitation.

2. *Compressibility Effect on Separation Control*

The location of the shock wave at compressible speeds coincides with the location of the steep adverse pressure gradient over the highly convex area of the model that causes separation at low Mach numbers. At $M = 0.65$ the shock turns the flow subsonic just upstream of separation because $C_{p,\mathrm{crit}} = -1.01$ (Fig. 8, asterisk). The length of the baseline bubble at $M = 0.65$ is only slightly longer than its length at $M = 0.25$. The lengthening of the bubble is an indication of the lower mixing rate in the compressible shear layer because the mixing rate determines the rate at which the separated shear layer approaches the wall. The range of the available reduced frequencies, based on the length of the bubble (taken here also as $c/2$, Ref. 8) and on the freestream velocity, was 0.15–0.6. The effect of two of these frequencies was studied at an oscillatory momentum coefficient of $\langle c_\mu \rangle = 0.06\%$ (see Fig. 8), and the results indicate that $F^+ = 0.6$ is the most effective frequency of those tested for shortening the bubble. The receptivity of the separated shear layer, as indicated by C'_p at $x/c = 0.67$, is not frequency dependent, whereas $F^+ = 0.6$ is the most amplified above the bubble. A very weak unsteady upstream (of the slot) effect (that is, at $x/c = 0.2$) of the excitation was measured at $M = 0.65$ (C'_p in Fig. 8). This finding differs from our findings for low Mach numbers using low F^+ (Ref. 8, Fig. 8a). The reason for this effect is that the upstream acoustic propagating wave can not affect the region that is upstream of a supersonic flow.

The effect of increasing the excitation magnitude on the efficacy of active separation control at $M = 0.65$ is presented in Fig. 9. The strength of the shock wave increases with the excitation level, the mean bubble gets shorter, and the magnitude of $C'_{p\,\max}$ increases and it moves upstream (broken line, RHS ordinate in Fig. 9). Again, the unsteady excitation is not sensed upstream of the supersonic region (not shown), at $x/c = 0.2$ because C'_p there is unchanged.

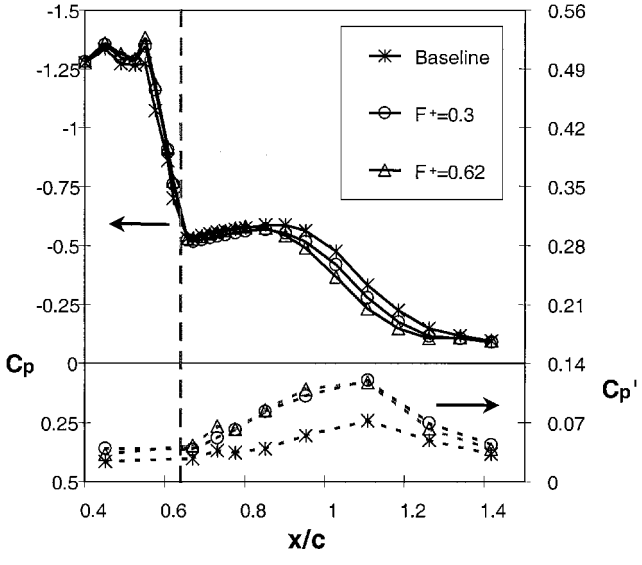

Fig. 8 Effects of frequency on baseline and controlled pressure distributions, $M = 0.65$, $R_c = 30 \times 10^6$, and $\langle c_\mu \rangle = 0.06\%$: ¦, $x/c = 0.64$ slot location.

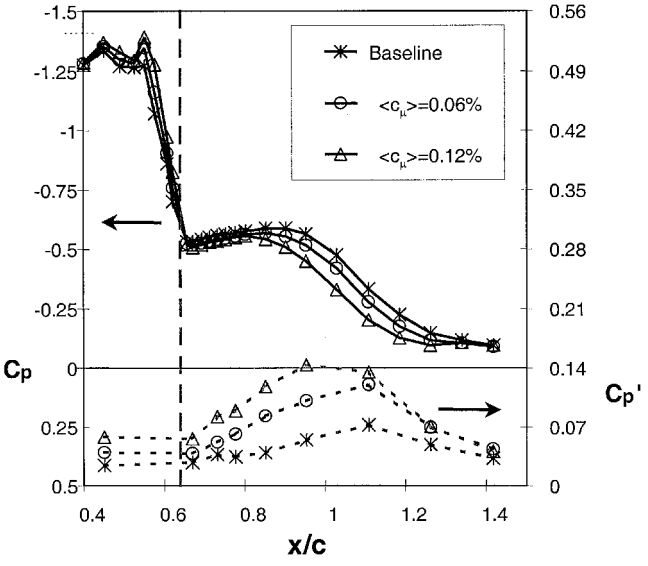

Fig. 9 Amplitude effect on baseline and controlled pressure distributions, $M = 0.65$, $R_c = 30 \times 10^6$, and $F^+ = 0.3$: ¦, $x/c = 0.64$ slot location.

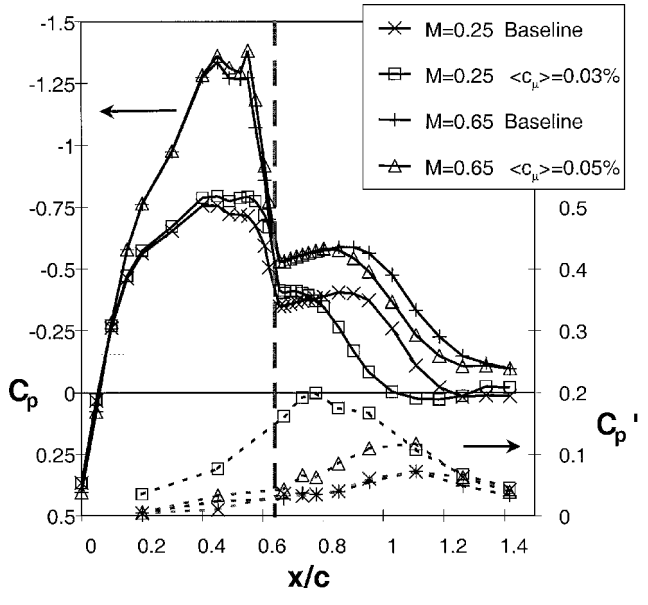

Fig. 10 Compressibility effects on baseline and controlled pressure distributions: $M = 0.65$, $R_c = 30 \times 10^6$, and $F^+ = 0.6$ and $M = 0.25$, $R_c = 16 \times 10^6$, and $F^+ = 0.8$.

An indication to the effectiveness of active separation control at different Mach numbers can be obtained by evaluating the reduction in the length of the separation bubble for a given $\langle c_\mu \rangle$ and F^+. This was performed by comparing mean and fluctuating pressures generated by $F^+ = 0.3$ and $\langle c_\mu \rangle = 0.05\%$ at $M = 0.65$ with those generated by $F^+ = 0.4$ and $\langle c_\mu \rangle = 0.03\%$ at $M = 0.25$, respectively (Fig. 10). The effects of the slightly different frequency and amplitude used at the two Mach numbers are not considered essential. Note also that the compressible separation occurs at different C_p and, downstream of reattachment, the C_p is not zero due to wall interference (see also Fig. 6). Therefore, the bubble pressure coefficients were normalized in the following manner:

$$C_{p,n} = \frac{C_p - C_{p,R,b}}{C_{p,s,b} - C_{p,R,b}} \tag{1}$$

to enable a clearer comparison. The effect of this scaling on the pressure distributions of the baseline bubbles can be seen in Fig. 11a. (Note that the pressure fluctuations C'_p were not scaled.) The scaling shows a slightly longer bubble at $M = 0.65$. The same scaling

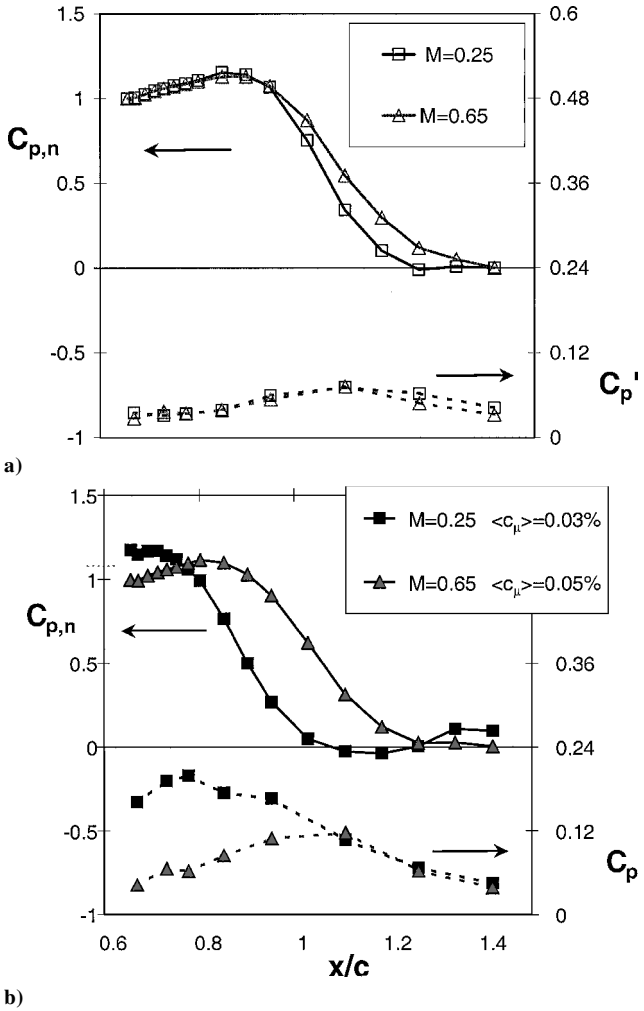

Fig. 11 Compressibility effects on a) baseline and b) controlled pressure distributions using the $x/c = 0.64$ slot, normalized according to text: $M = 0.65$, $R_c = 30 \times 10^6$, and $F^+ = 0.6$ and $M = 0.25$, $R_c = 16 \times 10^6$, and $F^+ = 0.8$.

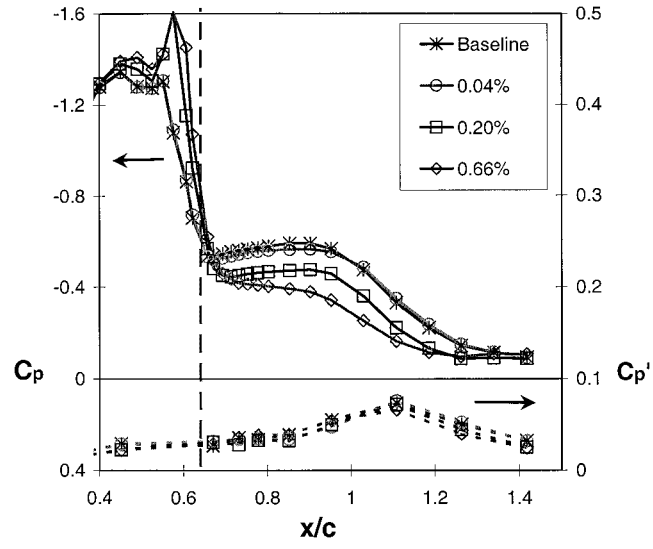

Fig. 12 Effect of steady blowing on the pressure distributions: $M = 0.65$, $R_c = 30 \times 10^6$, and slot $x/c = 0.64$, (blowing C_μ in legend).

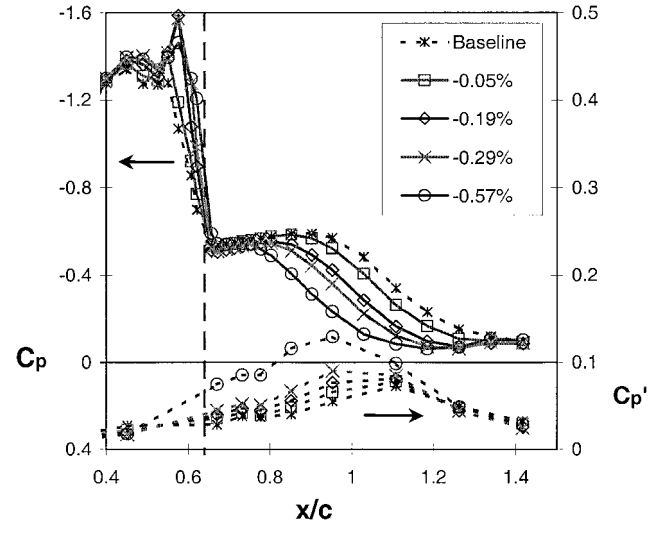

Fig. 13 Effect of steady suction on the pressure distributions: $M = 0.65$, $R_c = 30 \times 10^6$, slot $x/c = 0.64$ (negative C_μ in legend indicates suction).

was applied to the controlled bubble C_p (Fig. 11b). Whereas at $M = 0.25$, $C_{p,s}$ increased due to the control, at $M = 0.65$, $C_{p,s}$ is unchanged. The initialization of the pressure recovery takes place further downstream at the higher Mach number, that is, at $x/c = 0.75$ for $M = 0.25$ and only at $x/c = 0.9$ for $M = 0.65$. A threefold increase in $C'_{p\,\max}$ (compared to the baseline) and a forward movement of $C'_{p\,\max}$ to $x/c = 0.8$ can be observed at $M = 0.25$, whereas at $M = 0.65$, $C'_{p\,\max}$ increases by a factor of only two, and it moves forward only to $x/c = 1.05$. Based on the data of Fig. 11, it could be concluded that at compressible flow conditions, periodic excitation is less effective than at incompressible flow, at least in shortening the bubble using low F^+ that is introduced from the $x/c = 0.64$ slot. As will be shown in the following section, the effectiveness of steady mass flux in shortening the baseline bubble is also reduced at $M = 0.65$.

Steady mass flux was applied to control separation at compressible speeds, and its effectiveness is evaluated at $M = 0.25$ and 0.65 and compared to the efficacy of unsteady excitation. Figure 12 presents the mean and fluctuating wall pressure distributions at $M = 0.65$ due to the application of steady blowing from the $x/c = 0.64$ slot. Only a weak response can be seen for blowing at $c_\mu < 0.2\%$, similar to the results found at low Mach numbers. For $c_\mu > 0.2\%$, separation moves downstream, causing flow acceleration upstream and increasing the strength of the shock wave. Reattachment does not move forward because C'_p does not increase and $C'_{p\,\max}$ stays at the same location.

Steady suction was also used to control the bubble at $M = 0.65$ and the corresponding pressure distributions are presented in Fig. 13.

Note that suction is indicated by negative c_μ. The data presented in Fig. 13 demonstrates that the response to steady suction is gradual and is mainly manifested as a shortening of the bubble through increased flow unsteadiness and indicated by the increased wall pressure fluctuations downstream of separation. The strength of the shock wave increases, presumably due to the suction that induces acceleration upstream of the slot. The pressure at separation does not change considerably. Reattachment moves upstream as indicated by the upstream movement of $C'_{p\,\max}$, the more upstream beginning of the pressure recovery region and the more upstream reestablishment of zero pressure gradient flow.

Figure 14a presents a comparison of steady and periodic momentum transfer effects on the aerodynamic moment coefficient C_m measured at $M = 0.25$ and 0.65. Similar trends could be seen in the moment data regardless of the Mach number. Suction is more effective than blowing in modifying the moment, and the response to changes in the suction level is gradual over the entire c_μ range. The C_m is mainly indicative of a shortening of the bubble and its modification is important for guidance and control purposes. Steady blowing is less effective than steady suction or periodic excitation in modifying C_m. Figure 14b presents the effect of compressibility on the modification of the form drag C_{dp} by steady and periodic momentum transfer. Because the form drag is mainly affected by

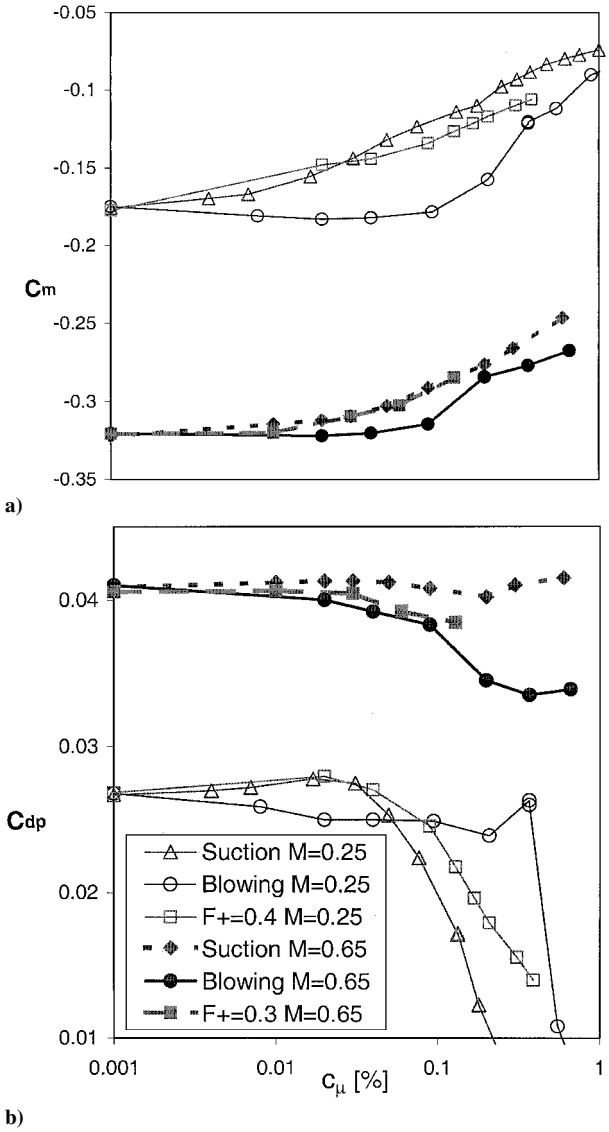

Fig. 14 Effect of steady and periodic momentum addition on a) the moment coefficient (legend as in b) and b) form drag: $M = 0.65$ and $R_c = 30 \times 10^6$ and $M = 0.25$, $R_c = 16 \times 10^6$, and $x/c = 0.64$ slot used.

changes in the pressures on the highly sloped areas of the model, one should not be surprised to find that the form drag at $M = 0.65$ is not affected as it was at $M = 0.25$ because the modifications of C_p at the lee side of the model are smaller (Fig. 11). Suction is not effective in reducing the form drag because the mean pressure at separation does not increase with the increase in c_μ (Fig. 13). Blowing and periodic excitation are more effective at reducing the form drag because the pressures at separation increase with the blowing or excitation c_μ (Fig. 12). Furthermore, blowing generates a favorable effect for $c_\mu < 0.1\%$, whereas at low Mach numbers it becomes effective only for $c_\mu > 0.2\%$.

The modification of the integral parameters due to the application of periodic excitation are compared to the effects due to the application of steady mass flux in Figs. 14a and 14b. The compared reduced frequencies, $F^+ = 0.4$ at $M = 0.25$ and $F^+ = 0.3$ at $M = 0.65$, are located near the lower limit of the effective frequencies for separation control. The data indicate that periodic excitation using low F^+ is as effective as steady suction in modifying the C_m at compressible speeds, whereas it was less effective at $M = 0.25$. The reduced frequency $F^+ = 0.3$ at $M = 0.65$ follows the form drag blowing data very closely, whereas steady suction is ineffective in modifying C_{dp} at $M = 0.65$. A comparison of the pressure distributions measured in the presence of periodic excitation with those generated by the application of steady mass flux, using the same C_μ (<0.1%, data not shown) indicates that both $F^+ = 0.3$ and 0.6 are more effective in shortening the bubble than steady suction. It could be concluded that the efficacy of periodic excitation in modifying the integral parameters is not reduced by compressibility.

D. Effects of Excitation Slot Location

The effect of the relative location between the excitation slot and the boundary-layer separation region was studied using two alternative blowing slot locations, that is, $x/c = 0.59$ and 0.64 at $M = 0.25$ and 0.65. Separation always occurred at $x/c \approx 0.65$, regardless of the Reynolds number or the Mach number. It was previously shown[8] that the location of the blowing slot did not alter the baseline separation to a measurable extent, at low Mach numbers, but it did affect the shock wave and the subsequent separation at compressible speeds, as will be shown here.

A range of steady suction rates was applied from the two alternative slots at $M = 0.25$ and $R_c = 21 \times 10^6$. The normal force (LHS ordinate) and the form drag (RHS ordinate) coefficients, shown in Fig. 15, demonstrate that when suction is applied from the $x/c = 0.59$ slot it has a gradual, but small, effect on the integral parameters. Suction that is applied from the $x/c = 0.64$ slot has a negligible, or even detrimental, effect on C_{dp} for $c_\mu < 0.05\%$. The form drag is gradually and very effectively eliminated using higher suction levels ($C_{dp} = 0$ for $c_\mu \sim 0.6\%$) that are applied from the $x/c = 0.64$ slot. This finding indicates that the boundary-layer thinning is only marginally effective in delaying separation on highly curved surfaces.

The effect of the slot location on the efficacy of periodic excitation ($F^+ = 0.8$) or steady suction, with increasing c_μ, in reducing the form drag, is shown in Fig. 16. The data indicate that introducing periodic excitation from the $x/c = 0.59$ slot increases the form drag for the entire available range of $\langle c_\mu \rangle$, whereas steady suction that was introduced from the $x/c = 0.59$ slot has a weak but gradual and favorable effect of drag reduction (Fig. 15). This weak effect presumably occurs due to thinning of the boundary layer upstream of separation. Introducing periodic excitation from the $x/c = 0.64$ slot is significantly more effective than introducing it from the $x/c = 0.59$ slot. It has a similar, though weaker, effect on steady suction that is applied from the $x/c = 0.64$ slot. The great sensitivity to a slot location change of only 5% chords is attributed to the highly curved surface in the separation region on the current model.

Baseline and controlled C_p and C'_p, distributions where periodic excitation with $\langle c_\mu \rangle \approx 0.06\%$ and $F^+ = 0.8$ emanates from either one of the slots, are presented in Fig. 17a. The baseline pressure distributions indicate that, whereas the $x/c = 0.59$ slot (its location indicated by a thick dashed–dotted line) is located at the beginning

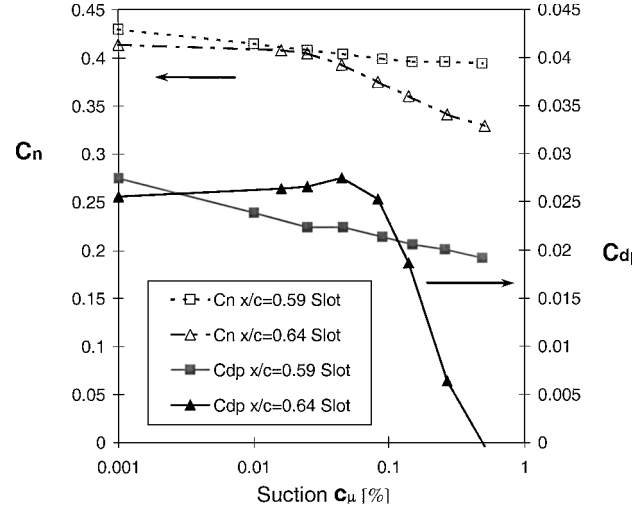

Fig. 15 Effect of the slot location on the normal force (C_n, LHS ordinate) and on the form drag (C_{dp}, RHS ordinate) using suction for control: $M = 0.25$ and $R_c = 21 \times 10^6$.

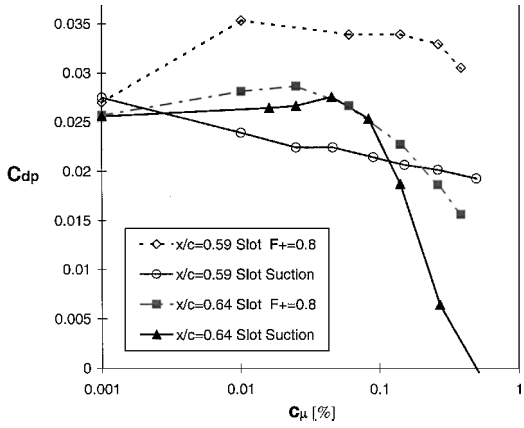

Fig. 16 Effect of the slot location on the form drag reduction using steady suction and periodic excitation for control: $M = 0.25$ and $R_c = 21 \times 10^6$.

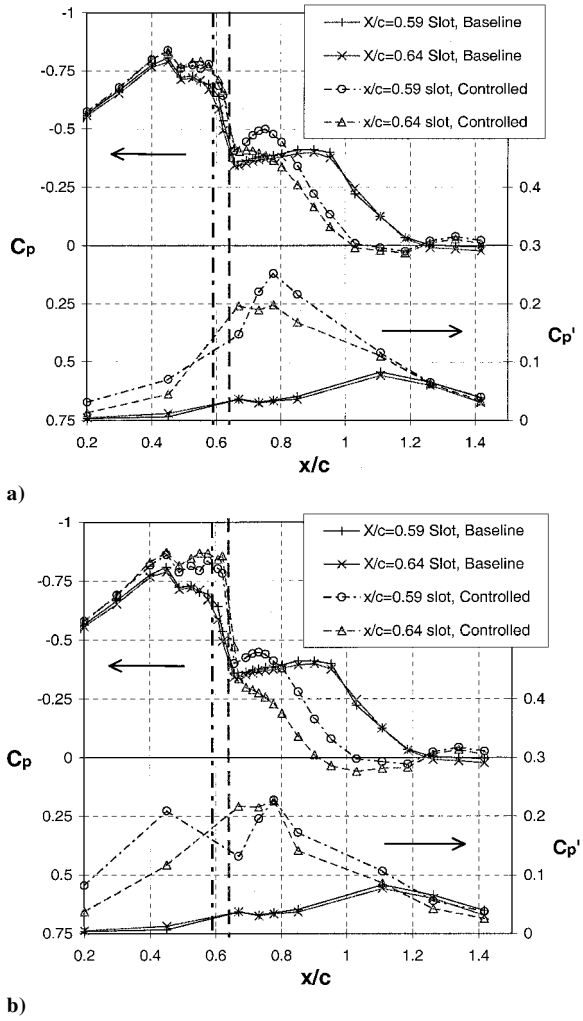

Fig. 17 Effect of the slot location (indicated by the vertical thick broken lines with the same style as the lines connecting data points) on C_p and C'_p using $F^+ = 0.8$ for control with a) $\langle c_\mu \rangle = 0.06\%$ and b) $\langle c_\mu \rangle = 0.38\%$ $M = 0.25$ and $R_c = 21 \times 10^6$.

of the baseline pressure recovery, the $x/c = 0.64$ slot (thick dashed line) is located just upstream of separation. The data show that low amplitude excitation (Fig. 17a) promotes separation at a slightly lower C_p at $x/c = 0.65$, regardless of the excitation slot location. The $x/c = 0.64$ excitation causes immediate turning of the shear layer toward the wall, whereas the $x/c = 0.59$ excitation increases the spreading rate of the shear layer (because the flow above the bubble continues to accelerate). This is accompanied by a very strong amplification of the wall C'_p (for $0.65 < x/c < 0.8$). The pressure recovery rate of the excited flow using the $x/c = 0.59$ slot for $x/c > 0.75$ is larger than that of the $x/c = 0.64$ slot excitation. This leads to reattachment at similar locations, about one separation height downstream of the secondary $C'_{p\,\max}$, that is positioned at $x/c = 0.78$. When the excitation emanates from the $x/c = 0.59$ slot, its effect upstream of the slot is stronger.

Significant differences in the effectiveness of high-amplitude periodic excitation, using $\langle c_\mu \rangle = 0.38\%$ and $F^+ = 0.8$ that emanates from the two alternative excitation slots, can be seen in Fig. 17b. A sixfold increase in the magnitude of the excitation does not significantly affect the average controlled C_p when the excitation is introduced from the $x/c = 0.59$ slot. Because the excitation was introduced 5–6% chord upstream of separation, the excitation level decayed considerably in the attached region of the boundary layer. The spatial resolution of the unsteady pressure transducers is too coarse to quantify this effect. The $x/c = 0.64$ excitation has almost twice the magnitude of the $x/c = 0.59$ excitation immediately downstream of separation (that is, C'_p at $x/c = 0.67$, Fig. 17b). Separation is delayed using the $x/c = 0.64$ excitation, causing not only a thinner bubble (because separation occurs further downstream on the highly sloped area at the lee side of the model) but also a shorter bubble. As seen for the low $\langle c_\mu \rangle$ excitation, the unsteady upstream effect of the excitation is stronger when the $x/c = 0.59$ slot is used. The excitation C'_p saturated between the $x/c = 0.64$ slot and $x/c = 0.8$ whereas it was amplified over the same x/c region for $x/c = 0.59$ slot excitation. Note that the slot location has only a negligible effect on the baseline model pressures (Fig. 17).

The effects of steady suction with $c_\mu \sim 0.5\%$ that is applied from the two slot locations are shown in Fig. 18. Suction at $c_\mu \sim 0.5\%$ accelerates the flow upstream of the active slot, regardless of its location. Whereas suction that is applied from the $x/c = 0.59$ slot removes a relatively thin boundary layer, the slot at $x/c = 0.64$ helps the thicker turbulent boundary layer overcome the separation ordained convex area. Interestingly, the flow downstream of the $x/c = 0.64$ slot continues to decelerate when suction is applied. This will presumably be the case as long as the unsteady stagnation downstream of the slot is not brought up to the rear edge of the slot. At a suction level of $c_\mu \sim 0.5\%$, only a very small separation bubble exists between $0.7 < x/c < 0.8$. Reattachment occurs at $x/c = 0.85$ and 1.0 for the $x/c = 0.64$ and 0.59 slots, respectively, as inferred from the location of $C'_{p\,\max}$. These results suggest that suction will be very effective in separation control when applied immediately downstream of highly convex areas.

The incompressible data that were presented in this section clearly demonstrate that control should be applied upstream of separation and as close as possible to it, regardless of the control method.

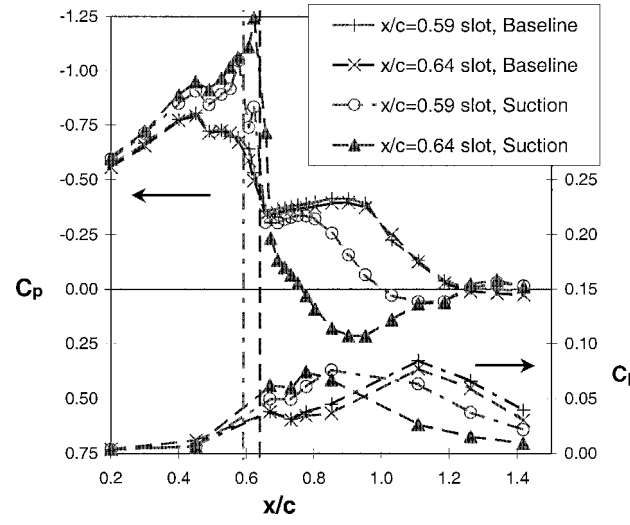

Fig. 18 Effect of the slot location on C_p and C'_p using steady suction with $c_\mu = -0.5\%$ for control: $M = 0.25$ and $R_c = 21 \times 10^6$ (common line style for slot locations and lines connecting data points).

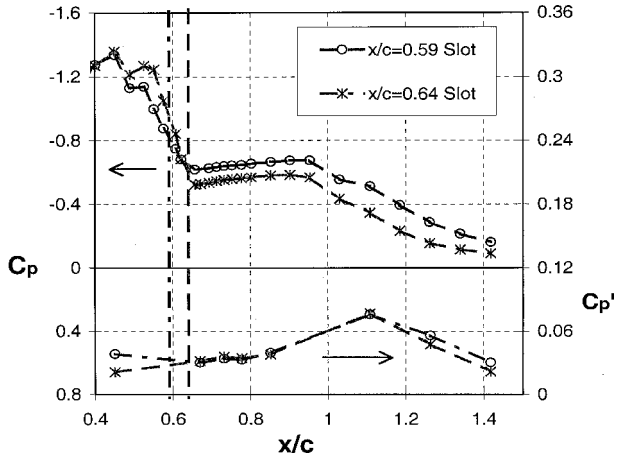

Fig. 19 Slot location effect on baseline C_p and C'_p: $M = 0.65$ and $R_c = 29 \times 10^6$ (common line style for slot locations and lines connecting data points).

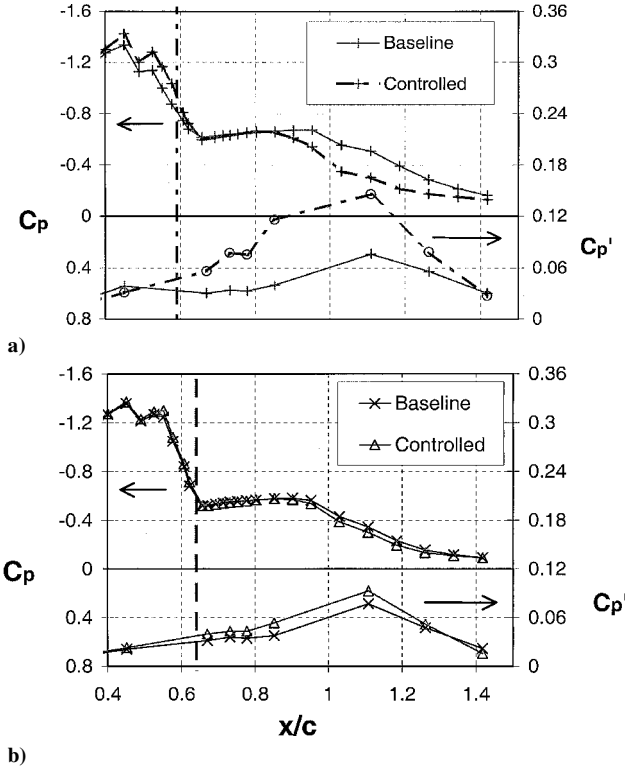

Fig. 20 Effect of slot location on the model pressures using $F^+ = 0.62$ and $\langle c_\mu \rangle = 0.03\%$ for control, $M = 0.65$, and $R_c = 29 \times 10^6$: a) $x/c = 0.59$ slot and b) $x/c = 0.64$ slot: ¦, slot location.

This is especially important on small radius of curvature convex surfaces.

In contrast to low Mach numbers, the mere presence of a slot alters the shock wave and separation location at compressible speeds (Fig. 19). The $x/c = 0.59$ slot, which is positioned under the mean shock position, causes an unsteady motion in the shock position (indicated by the increased unsteadiness at $x/c = 0.45$) that is manifested as weaker pressure recovery across the shock and separation at a lower C_p.

The incompressible data discussed in connection to Figs. 15–18 clearly indicate that the slot located at $x/c = 0.64$ is more effective than the slot located in $x/c = 0.59$ at low Mach numbers. At $M = 0.65$, however, the introduction of periodic excitation from the $x/c = 0.59$ slot is significantly superior to its introduction from the $x/c = 0.64$ slot, with identical F^+ and $\langle c_\mu \rangle$ (Figs. 20a and 20b). The increased upstream suction peak, the increased C'_p downstream of the slot, the reduced C'_p upstream of the slot, the upstream motion of $C'_{p\,\max}$, and the healthier pressure recovery above the bubble, indicate the increased effectiveness of the excitation that is introduced under the shock rather than downstream of it, that is, $x/c = 0.59$ rather than 0.64.

A physical interpretation of the aforementioned observations could hopefully be obtained from unsteady numerical simulation, using the data set provided in the present manuscript.

IV. Conclusions

Active separation control was applied to a carefully documented baseline flow at high Reynolds numbers. This paper describes several effects of compressibility and excitation slot location on the baseline and on the controlled flow. The baseline flow is fully turbulent so that laminar/turbulent transition does not baffle the data trends due to the active separation control. The Reynolds number has a very weak effect on the model pressure distributions, regardless of the Mach number. The spanwise uniformity of the wall pressures was found to be very good and improved as the separation was controlled using either steady suction or periodic excitation. Compressibility tends to elongate the separation bubble due to reduced mixing above the separated shear layer.

It was found that active control using periodic excitation is comparable to steady suction and significantly more effective than steady blowing, also at compressible speeds, as long as the modification of the integral parameters is considered. The capability of periodic excitation to shorten the separation bubble is reduced at compressible speeds, using similar reduced frequencies and excitation levels.

The effectiveness of the excitation slot located at $x/c = 0.64$ is significantly higher than the slot located at $x/c = 0.59$ at low Mach numbers. This is because the magnitude of the excitation considerably decays in the attached region of the boundary layer and separation takes place at $x/c \approx 0.65$. At compressible speeds, the presence of the $x/c = 0.59$ excitation slot alters the pressure distributions and separation location. However, the effectiveness of the $x/c = 0.59$ slot, which is located under the shock wave, is greater than that located at $x/c = 0.64$, just downstream of the shock. The shock-wave location and the separation region are very close in the present geometry. This eliminates the possibility of introducing the excitation downstream of the shock and still upstream of separation.

Within the limited range of frequencies and amplitudes that the current excitation system and flow conditions allowed, it was found that the highest F^+ (0.6) and the largest $\langle c_\mu \rangle$ (0.12%) were below the optimal, and saturation was not reached.

Acknowledgments

The experiment was performed while the first author held a National Research Council–NASA Langley Research Center research associateship. The authors would like to thank the following individuals for their substantial support of the research program: W. L. Sellers III, M. J. Walsh, R. D. Joslin, R. W. Wlezien, J. F. Barthelemay, B. L. Berrier, L. D. Leavitt, B. K. Stewart, G. C. Hilton, M. K. Chambers, L. Harris Jr., P. I. Tiemsin, J. Knudsen, P. T. Bauer, J. Thibodeaux, S. G. Flechner, J. T. Kegelman, and many other NASA employees and contractors, as well as D. Greenblatt for reviewing the manuscript.

References

[1]Betz, A., "History of Boundary Layer Control in Germany," *Boundary Layer and Flow Control*, Vol. 1, edited by G. V. Lachman, Pergamon Press, New York, 1961, p. 2.

[2]Nishri, B., and Wygnanski, I., "Effect of Periodic Excitation on Turbulent Flow Separation from a Flap," *AIAA Journal*, Vol. 36, No. 4, 1998, pp. 547–556.

[3]Seifert, A., Bachar, T., Koss, D., Shepshelovich, M., and Wygnanski, I., "Oscillatory Blowing, a Tool to Delay Boundary-Layer Separation," *AIAA Journal*, Vol. 31, No. 11, 1993, pp. 2052–2060.

[4]Seifert, A., Darabi, A., and Wygnanski, I., "Delay of Airfoil Stall by Periodic Excitation," *Journal of Aircraft*, Vol. 33, No. 4, 1996, pp. 691–699.

[5]Seifert, A., and Pack, L. G., "Oscillatory Control of Separation at High Reynolds Numbers," *AIAA Journal*, Vol. 37, No. 9, 1999, pp. 1062–1071.

[6]Seifert, A., and Pack, L. G., "Oscillatory Control of Shock-Induced Separation," *Journal of Aircraft*, Vol. 38, No. 3, 2001, pp. 464–472.

[7]Delery, J. M., "Shock Wave/Turbulent Boundary Layer Interaction and its Control," *Progress in Aerospace Sciences*, Vol. 22, 1985, pp. 209–280.

[8]Seifert, A., and Pack, L. G., "Active Flow Separation Control on a Wall-Mounted Hump at High Reynolds Numbers," *AIAA Journal*, Vol. 40, No. 7, 2002, pp. 1363–2372.

[9]Murthy, A. V., Johnson, C. B., Ray, E. J., Lawing, P. L., and Thibodeaux, J. L., "Studies of Sidewall Boundary Layer in the Langley 0.3-Meter Transonic Cryogenic Tunnel With and Without Suction," NASA TP-2096, 1983.

[10]Ladson, C. A., and Ray, E. J., "Evolution, Calibration, and Operational Characteristics of the Two-Dimensional Test Section of the Langley 0.3-Meter Transonic Cryogenic Tunnel," NASA TP-2749, 1987.

[11]Rallo, R. A., Dress, D. A., and Siegle, H. J. A., "Operating Envelope Charts for the Langley 0.3-Meter Transonic Cryogenic Wind Tunnel," NASA TM-89008, 1986.